



Published in final edited form as:

IEEE Trans Biomed Eng. 2010 October ; 57(10): 2572–2575. doi:10.1109/TBME.2010.2058109.

Depth-Resolved Blood Oxygen Saturation Assessment Using Spectroscopic Common-Path Fourier Domain Optical Coherence Tomography

Xuan Liu and

Department of Electrical and Computer Engineering, Johns Hopkins University, Baltimore, MD 21218 USA

Jin U. Kang[Member, IEEE]

Department of Electrical and Computer Engineering, Johns Hopkins University, Baltimore, MD 21218 USA

Xuan Liu: xliu35@jhu.edu; Jin U. Kang: jkang@jhu.edu

Abstract

Although spectroscopic optical coherence tomography (OCT) has been shown to be a promising method for measuring blood oxygen saturation with high-spatial resolution and accuracy, there are several technical issues that need to be addressed before it could become a practical method. In this letter, we have attempted to address two issues that could significantly improve the quantitative assessment of blood oxygen saturation level. First, we have implemented a spectral normalization technique to eliminate the spectral modulation induced by the wavelength–distance-dependent point spread function (PSF) of OCT's. Second, to reduce the spectral speckle noise due to the highly scattering blood, we have implemented a spatial low-pass filter to the 2-D OCT dataset consisting of spectra obtained at different lateral positions. We have assessed the effectiveness of these methods using common-path OCT system. Results showed that we were able to extract unambiguous depth-resolved, SO_2 -dependent spectroscopic information from 1-D and 2-D OCT images, which could be used to accurately assess the SO_2 level.

Index Terms

Oxygen saturation; spectroscopic optical coherence tomography (SOCT)

I. Introduction

Measurements of oxygen saturation have a variety of clinical applications. One of such applications of our interest is in monitoring the change of autoregulation and blood flow in the retina, which has been linked to several pathologic changes. Another useful application is to measure the oxygen saturation level of central venous at retina as an index of oxygen delivery to vital organs including brain [1], [2]. However, due to the ambiguity induced by the unknown optical-path length and the layered structure of retina, so far it has been challenging to precisely measure SO_2 in retina. Optical coherence tomography (OCT) may be used to remove such ambiguity, because OCT can resolve retinal layers with high-spatial resolution and can extract the spectroscopic properties of the sample simultaneously.

Correspondence to: Jin U. Kang, jkang@jhu.edu.

Color versions of one or more of the figures in this paper are available online at <http://ieeexplore.ieee.org>.

However, the high scattering in the blood and the surrounding tissues prevent accurate assessment of the SO_2 level in the blood. In recent years, several studies using OCT have demonstrated different methods that deal with the assessment of oxygen saturation level accurately [3]–[6]. The key to the SO_2 assessment is based on different absorption features of hemoglobin (Hb) and oxyhemoglobin (HbO_2), which can be measured spectroscopically using spectroscopic OCT (SOCT) [3]–[6]. Faber *et al.* measured the absorption spectra of Hb and HbO_2 in non-scattering diluted blood, and later, using highly scattering whole blood using SOCT [3], [4]. This has led to a conclusion that an accurate measurement of the scattering properties of blood is required to quantitatively assess SO_2 . Lu *et al.* reported the measurement of blood SO_2 by exponentially fitting the A-scans of the long- and short-wavelength ranges to extract overall blood attenuation coefficients in whole blood, which could provide an accurate assessment [5].

Although these preliminary studies showed promising results, they have neglected to satisfactorily address two significant problems that limit SOCT to be applied clinically in blood SO_2 measurement. The first difficulty comes from OCT system's point spread function (PSF), which has a wavelength dependency varying as a function of the distance between confocal and coherence gate of OCT when a tightly focused beam is used [7], [8]. To eliminate the spectral modification induced by OCT's PSF, a dynamic focusing technique was typically used to match the confocal gate and the coherence gate for the quantitative measurement of the tissue absorption [3], [4], [9]. With the dynamic focusing, Faber measured Hb and HbO_2 absorption using time-domain SOCT and the results of their study were in good agreement with published experimental data and theoretical model [3]. However, the main disadvantage of dynamic focusing is that the data acquisition rate is extremely slow ~ 1 Hz/A-scan, because the distance between the sample and the focusing lens of the sample arm had to be adjusted mechanically to make sure that the coherence gate and the confocal gate overlapped for every pixel in an A-scan. The second problem of using OCT for the SO_2 measurement comes from the prevalent existence of multiple scattering. As a result of multiple scattering, a speckle pattern tends to form and randomizes the spectrum. The speckle induced random backscattering profile is inevitable when imaging highly scattering whole blood and this makes it difficult to quantitatively extract accurate absorption coefficient from OCT signal. One of the solutions to this problem is to average multiple A-scans, which reduces the speckle noise. However, this further increases the data acquisition time [3]–[5].

In this study, we applied and analyzed methods to address these two problems. To eliminate the first problem, the wavelength–distance-dependent PSF of OCT, we implemented a spectral normalization technique based on the fact that the PSF can be measured in prior [8]. With the spectral normalization, we were able to obtain the accurate absorption spectra of deoxygenated and oxygenated diluted blood. The results showed an unambiguous high-spectral resolution crossover behavior of Hb and HbO_2 absorption spectra. The second problem, speckle noise, creates a significant problem when one tries to assess SO_2 from 2-D OCT images of whole blood. We have implemented and analyzed the effectiveness of using a spatial low-pass filtering on the localized spectra in reducing the speckle noise. The results showed the unambiguous crossover behavior of Hb and HbO_2 absorption spectra as well. Without dynamic focusing and extensive averaging, we have significantly increased the data acquisition speed for SO_2 measurement. We have assessed these methods using a common-path Fourier-domain OCT (CP FD OCT). In CP FD OCT, the reference and sample signals share the same probe arm; therefore, the whole system can be compact, rugged, cost-effective, and free of system dispersion [10].

II. Theory

The hemoglobin oxygen saturation level SO_2 is defined as the percentage of HbO_2 over total hemoglobin. Assuming that Hb and HbO_2 are the only chromophores in the blood [11], we can express blood's absorption coefficient as follows:

$$\alpha = C[\varepsilon_{Hb}(\lambda)(1 - SO_2) + \varepsilon_{HbO_2}(\lambda)SO_2]. \quad (1)$$

In (1), ε_{Hb} and ε_{HbO_2} denote Hb and HbO_2 's extinction coefficients, which depend on wavelength, as shown in Fig. 1 [12]; C denotes the total concentration of hemoglobin. As shown in (1), blood's absorption coefficient has a functional wavelength dependence that changes as SO_2 changes. Such a property is used to measure blood SO_2 .

In this study, the blood absorption property is extracted from interferograms detected by CP FD OCT. The interferogram can be expressed as follows [13]:

$$\begin{aligned} I_{OCT}(k) &= \int S_0(k)H_S(k, l)M(k, l)\cos(2kl)dl \\ &= \int U(k, l)\cos(2kl)dl. \end{aligned} \quad (2)$$

In (2), k is wavenumber ($k = 2\pi/\lambda$) and l indicates the distance between the reference plane and the sample slice; $S_0(k)$ indicates the source spectrum; $H_S(k, l)$ is the axial PSF of OCT system; and $M(k, l)$ denotes the spectral modulation induced by sample and we can deduce blood SO_2 from $M(k, l)$.

A-scan $i_0(l)$ is obtained by inverse Fourier transformation

$$i_0(l) = F^{-1}[I_{OCT}(k)]. \quad (3)$$

An estimation of $U(k, l)$ can be derived from Morlet wavelet transformation

$$\widehat{U}(k, l) = \left| F \left\{ i_0(l) \exp \left[-4 \ln 2 \frac{(l - l_0)^2}{L^2} \right] \right\} \right|. \quad (4)$$

In (4), l_0 indicates the center of the Gaussian window; so that it extracts the localized spectroscopic properties of the sample from this demodulation, o is to downshift the frequency by L indicating the full-width at half-maximum (FWHM) of the Gaussian window, which determines the spatial resolution of this analysis and F indicates Fourier transformation. Please note that there exists a tradeoff between spatial and spectral resolution in such time-frequency analysis, and the spectral resolution is inversely proportional to L .

As seen from (2) and (4), it requires us to know $H_S(k, l)$ and $S_0(k)$ in prior to extract $M(k, l)$ for the deduction of blood SO_2 .

III. Apparatus and Material

The schematic of our CP FD OCT is shown in Fig. 2(a). The broadband light gets coupled into one input port of a 50/50 fiber optic coupler and exits through one of the coupler's

output port, which is connected to a single-mode fiber serving as both sample and reference arm. The reference signal is obtained from the partial reflection at the distal end of the probe arm. The reference and the sample signal couple back to the probe arm and interfere. The light beam that exits the other input port of the coupler is detected by a spectrometer with a wavelength band from 700 to 890 nm, and has a spectral resolution of 0.1 nm. To obtain enough bandwidth that covers the absorption features of Hb and HbO₂ around 800 nm, two superluminescent emission diodes (SLED) from Exalos are multiplexed to serve as a broadband source and the source spectrum is shown in Fig. 2(b). The SLEDs' central wavelengths and bandwidths are 780 and 25 nm, and 810 and 30 nm, respectively. We used sheep blood (Hemostat Laboratories) that was defibrinated mechanically as our blood sample. To show that our SOCT can differentiate the oxygenation status of blood, we prepared the blood to be either fully oxygenated or deoxygenated. To fully oxygenate the blood, we simply placed the blood sample in the air. Calculating the oxygen saturation level according to the blood dissociation curve [15], we estimated that the SO₂ is greater than 99.6% when placing the blood in the air. In this calculation, we assumed the temperature of 25 °C; the partial pressures of oxygen and carbon dioxide are 160 and 0.22 mmHg, respectively; the pH value equals 7.4. In order to repel oxygen from hemoglobin and achieve 0% SO₂ level, we added more than 10 mg sodium hydrosulfide into 5 mL blood, which is sufficient to maintain the blood at 0% SO₂ for 30 min based on the experimental data in [14]. Assuming deoxygenated blood contains only Hb and oxygenated blood contains only HbO₂ as chromophore, the absorption spectra of deoxygenated and oxygenated blood should correspond to the absorption spectra of Hb and HbO₂, as shown in Fig. 1.

IV. Experiments and Results

We used the setup shown in Fig. 3(a) to test our spectral normalization method and assess the oxygen saturation in diluted blood from 1-D OCT signal. The probe arm of our CP FD OCT consisted of a 10× microscopic objective lens, a glass cuvette with a 1-mm-thick lumen, and a mirror. To minimize the scattering induced spectral modulation, we diluted the blood sample and derived the OCT signal in this experiment from light reflected by two specular surfaces, which were the mirror and the lower glass–air boundary of the cuvette. In order to form the interference pattern, it requires a delay between the mirror surface and the cuvette. We achieved this by tilting the cuvette several degrees with regard to the mirror surface, while gluing them together using optical epoxy. Before imaging, we adjusted the lateral position of the sample to make sure the epoxy did not block the optical path of incident beam. We first filled the cuvette with water to obtain an interferometric spectrum for normalization. Afterward, we filled the glass cuvette with diluted oxygenated blood and deoxygenated blood to induce SO₂-dependent absorption.

Using (3) to process the measured interferograms, we have obtained OCT A-scans that had one signal peak due to the interference between mirror and the lower glass–air boundary of the cuvette. Using a 25 μm FWHM Gaussian window that centered at the coherence peak, we calculated the localized spectra with (4) and the spectral resolution of this analysis was 11 nm. Water has low absorption, and therefore, $\hat{U}(k, l)$ obtained from water is simply the product of source spectrum $S_0(k)$ and OCT's PSF $H_S(k, l)$. With the sample arm immobilized, we assumed the delay between interfering light fields in all the three measurements (water, oxygenated, and deoxygenated blood) were the same and the confocal properties stayed the same as well; therefore, the spectra were modulated by an identical PSF. As a result, we were able to use the spectrum obtained from water measurement to normalize spectra obtained from blood. We divided the spectra obtained from blood (oxygenated or de-oxygenated) with the one obtained from water to remove the spectral modulation of source spectrum and OCT's PSF, so that we were able to obtain the spectral modulation induced by blood $M(k, l)$. Assuming absorption follows Beer's law, we were

able to obtain the wavelength-dependent absorption of blood by taking the logarithm of the normalized spectra. Results were shown in Fig. 3(b). To demonstrate that it is necessary to remove the PSF in obtaining the absorption spectra, in Fig. 3(c), we showed the absorption spectra of blood that were obtained by normalization with the source spectrum, but without OCT's PSF. It is worth mentioning that the absorption spectra in Fig. 3(b) and (c) were further normalized with their values at the isosbestic wavelength, and multiplied by $\varepsilon(\lambda_{iso})$ ($\sim 780\text{M/cm}$) based on the value in [12]; for elimination, the impact of the hemoglobin concentration and the optical path length, as well as for the convenience to compare with result shown Fig. 1. By eliminating effect induced by OCT's PSF through spectral normalization, Fig. 3(b) clearly shows the crossover behavior of Hb and HbO₂ absorption: the absorption of oxygenated blood increases as wavelength and the absorption of deoxygenated blood decreases as wavelength. However, in Fig. 3(c), we are not able to observe such crossover behavior of Hb and HbO₂.

Although results in Fig. 3(b) are highly promising, a clinical relevant setup will be different from the setup in Fig. 3(a) in two aspects. First, in a practical situation, the spectrum of reference light is independent from sample's spectroscopic properties. Second, when imaging a blood sample *in situ*, the signal light is backscattered by highly scattering blood and speckle tends to form and randomize the spectra, which makes it extremely challenging to measure SO₂ using OCT in scattering blood.

To assess SO₂ and obtain 2-D OCT image simultaneously from a highly scattering blood sample, we used a single-mode fiber as probe in our next setup and scanned the single-mode fiber probe above the blood sample with a step motor. We cleaved the fiber tip in right angle to obtain the reference light from the partial reflection of the fiber tip. The sample was prepared by placing a drop of undiluted blood (oxygenated or deoxygenated) on a glass cover slide and a thin blood film was formed on the surface of the glass slide. We scanned the probe across the edge of the blood film and the obtained 2-D OCT images are shown in Fig. 4(a) (oxygenated blood) and (b) (deoxygenated blood), in which the ramp-shaped blood films, as well as the upper and lower boundaries of the glass slide are visible. However, the difference in the oxygen saturation status does not induce any observable difference in the OCT images.

To extract blood's spectroscopic property that is correlated with SO₂, we studied the spectra originated from the upper surface of the glass slide, which is either the interface between glass and air, or the interface between glass and blood. When there is blood along the optical path, the light reflected by the upper surface of glass slide would have a spectrum modulated by the blood. To reduce the speckle noise, we spatially filtered the 2-D dataset consisting of spectra obtained at different lateral positions. The kernel of the filtering is a 1-D rectangular function, which effectively averages 15 spectra. Afterward, we obtained A-scans using (3) from the averaged spectra. We identified the signal peaks corresponding to the upper surface of the glass slide from the A-scans. Then, we used (4) with a 25- μm FWHM Gaussian window to extract the localized spectra from the A-scans. The resultant spectra were denoted as $U(\lambda, l_x)$, in which l_x indicates the lateral position. It is worth mentioning that although we did not use any focusing lens in front of the sample, as in Fig. 3(a), the light-coupling efficiency of the single-mode fiber depends on wavelength, as well as the distance between the reference plane and sample slice. As a result, the concept of "PSF" was still valid for this experiment in which a single-mode fiber was used as probe and the PSF had a wavelength-distance dependency. To obtain a baseline spectrum, we averaged the first 50 spectra corresponding to the beginning part of OCT image and denoted the result as $U_0(\lambda)$. There was no blood absorption at the beginning of B-scan; as a result, $U_0(\lambda)$ approximately equaled the product of OCT's PSF and the source spectrum, and thus could be used as a baseline. We thereafter normalized all the obtained $U(\lambda, l_x)$ with $U_0(\lambda)$ to remove OCT's

PSF and the source spectrum. The normalized spectra were denoted as $M(\lambda, l_x)$. A Gaussian filter with FWHM of $25 \mu\text{m}$ was further applied to $M(\lambda, l_x)$ along the lateral scanning dimension l_x to reduce the variation between spectra obtained from different lateral positions. $M(\lambda, l_x)$ obtained from measuring oxygenated and deoxygenated blood are shown in Fig. 5(a) and (b) in which the data range are converted to $[0, 1]$. Each column in Fig. 5(a) and (b) represents a spectrum with regard to a lateral position and the spectrum was originated from the upper surface of glass slides. When there is blood absorption, Fig. 5(a) has a larger spectral intensity in the shorter wavelength range, while Fig. 5(b) has a larger spectral intensity in the longer wavelength range. These results correlate well with the absorption behavior of HbO_2 and Hb, because HbO_2 has a smaller absorption coefficient in shorter wavelength range and the opposite is true for Hb. For each spectrum in Fig. 5(a) and (b), we averaged the spectral intensity within long- (819–848 nm) and short- (771–792 nm) wavelength bands. The chosen wavelength bands are either longer or shorter than the isosbestic point of the HbO_2 and Hb absorption spectra (800 nm). As a result, the averaged spectral intensities can reveal the crossover behavior of Hb and HbO_2 absorption. Moreover, our broadband source has a larger spectral intensity in the wavelength ranges that we chose, therefore a better signal-to-noise ratio may be obtained. We show the averaged intensity versus lateral position in Fig. 5(c) and (d) from which the crossover behavior of blood absorption can also be observed. The black circles in Fig. 5(c) and (d) indicate the edge of the blood film. Moreover, as seen from Fig. 5(c) and (d), the difference between spectral intensity in long- and short-wavelength range increases along with the thickness of the blood layer, which indicates the cumulative effect of absorption: with a larger interaction length, there is a larger absorption and a larger modulation in spectral shape.

V. Discussion and Conclusion

Signal attenuation in blood is due to both absorption and scattering. Since the scattering coefficient is much larger than absorption coefficient, accurately extracting absorption spectrum of blood is difficult. Nevertheless, we have extracted and observe the unambiguous crossover behavior of Hb and HbO_2 absorption spectra by applying both spectral normalization technique and spatial low-pass filtering.

The assessment was done using common-path-based SOCT with either fully oxygenated or fully deoxygenated blood. A spectral normalization technique was implemented to remove the spectral modulation of OCT's PSF and a spatial low-pass filtering was applied to reduce the speckle noise. Spectroscopic results obtained from 1-D and 2-D OCT data show good correlation with blood's oxygen saturation level. By using spectral normalization and spatial filtering to replace dynamic focusing and extensive averaging, the acquisition for SO_2 assessment could be done in real time and limited only by the time required to obtain a conventional OCT image.

Acknowledgments

This work was supported in part by the National Institutes of Health under Grant BRP 1R01 EB, Grant 007969–01, and Grant R21 1R21NS063131–01A1.

References

1. Harris A, Dinn RB, Kagemann L, Rechtman E. A review of methods for human retinal oximetry. *Ophthalmic Surg Lasers Imaging* 2003;34(2):152–164. [PubMed: 12665234]
2. Ramella-Roman JC, Mathews SA, Kandimalla H, Nabili A, Duncan DD, D'Anna SA, Shah SM, Nguyen QD. Measurement of oxygen saturation in the retina with a spectroscopic sensitive multi aperture camera. *Opt Exp* 2008;16:6170–6182.

3. Faber DJ, Mik EG, Aalders MCG, van Leeuwen TG. Light absorption of (oxy-)hemoglobin assessed by spectroscopic optical coherence tomography. *Opt Lett* 2003;28:1436–1438. [PubMed: 12943083]
4. Faber DJ, Mik EG, Aalders MCG, van Leeuwen TG. Toward assessment of blood oxygen saturation by spectroscopic optical coherence tomography. *Opt Lett* 2005;30:1015–1017. [PubMed: 15906988]
5. Lu CW, Lee CK, Tsai MT, Wang YM, Yang CC. Measurement of the hemoglobin oxygen saturation level with spectroscopic spectral-domain optical coherence tomography. *Opt Lett* 2008;33:416–418. [PubMed: 18311277]
6. Kagemann L, Wollstein G, Wojtkowski M, Ishikawa H, Townsend KA, Gabriele ML, Srinivasan VJ, Fujimoto JG, Schuman JS. Spectral oximetry assessed with high-speed ultra-high-resolution optical coherence tomography. *J Biomed Opt* 2007;12:041212–041219. [PubMed: 17867801]
7. Izatt JA, Hee MR, Owen GM, Swanson EA, Fujimoto JG. Optical coherence microscopy in scattering media. *Opt Lett* 1994;19:590–592. [PubMed: 19844382]
8. van Leeuwen TG, Faber DJ, Aalders MC. Measurement of the axial point spread function in scattering media using single-mode fiber-based optical coherence tomography. *IEEE J Sel Top Quantum Electron* Mar/Apr;2003 9(2):227–233.
9. Hermann B, Bizheva K, Unterhuber A, Považay B, Sattmann H, Schmetterer L, Fercher A, Drexler W. Precision of extracting absorption profiles from weakly scattering media with spectroscopic time-domain optical coherence tomography. *Opt Exp* 2004;12:1677–1688.
10. Sharma U, Kang JU. Common-path optical coherence tomography with side-viewing bare fiber probe for endoscopic optical coherence tomography. *Rev Sci Instrum* 2007;78:113102-1–113102-4. [PubMed: 18052460]
11. Roggan A, Friebel M, Dörschel K, Hahn A, Müller G. Optical properties of circulating human blood in the wavelength range 400–2500 nm. *J Biomed Opt* 1999;4:36–46.
12. 2001. [Online]. Available: <http://omlc.ogi.edu/spectra/index.html>
13. Xu C, Carney P, Boppart S. Wavelength-dependent scattering in spectroscopic optical coherence tomography. *Opt Exp* 2005;13:5450–5462.
14. Briely-Sæbø K, Bjørnerud A. Accurate de-oxygenation of ex vivo whole blood using sodium Dithionite. *Proc Intl Sot Mag Reson Med* 2000;8:2025.
15. 2000. [Online]. Available: <http://www.ventworld.com/resources/oxydisso/dissoc.html>, 2000

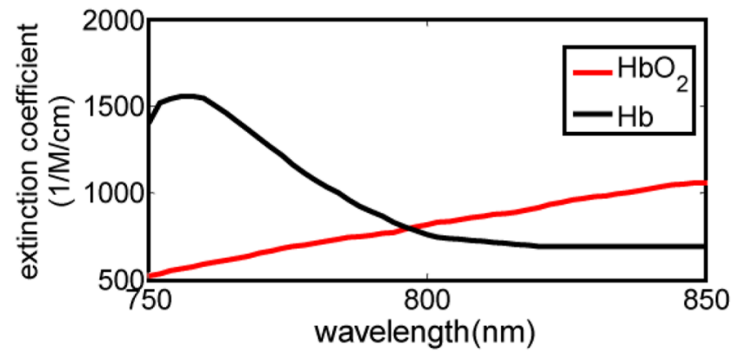


Fig. 1.
Molar extinction coefficient spectra of Hb and HbO₂.

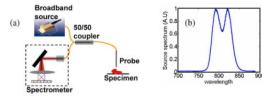


Fig. 2.
(a) Schematic of CP FD OCT. (b) Source spectrum.

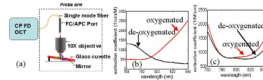


Fig. 3.

(a) Experimental setup for blood absorption measurement. (b) Absorption spectra of oxygenated (red curve) and deoxygenated (black curve) blood that were normalized by source spectrum and OCT's PSF. (c) Absorption spectra of oxygenated (red curve) and deoxygenated (black curve) blood that were normalized with source spectrum only.

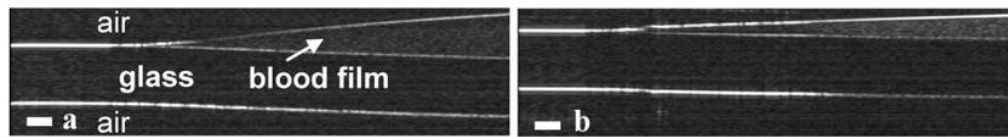


Fig. 4. OCT images of blood layer on the surface of a glass slide. (a) Oxygenated blood. (b) Deoxygenated blood. The bar represents 100 μm .

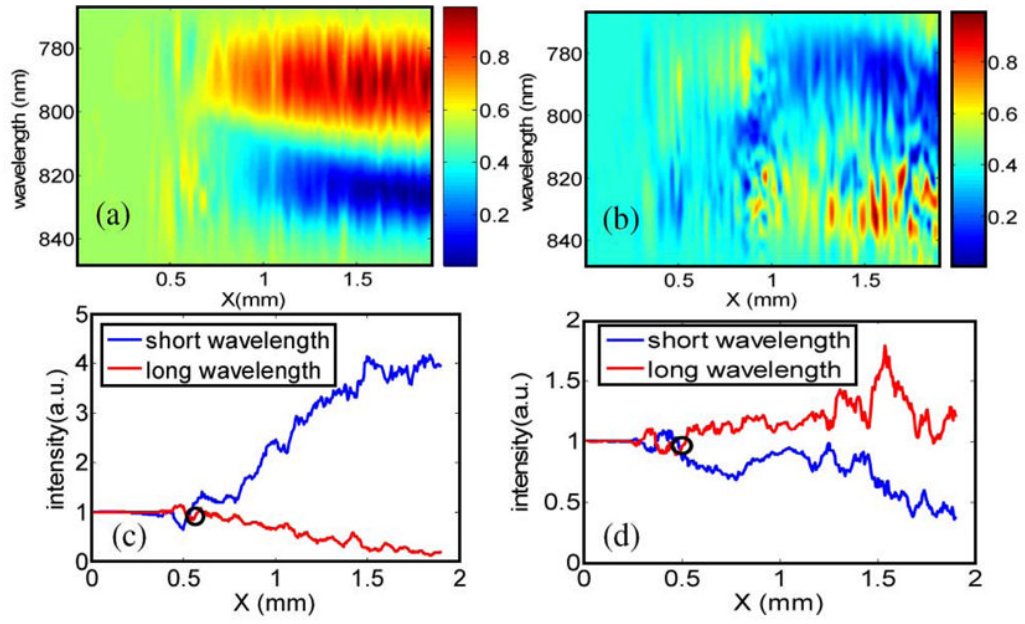


Fig. 5. Localized spectra versus lateral position, obtained from (a) oxygenated blood; (b) deoxygenated blood; average spectra intensity in long- and short-wavelength range versus lateral position, obtained from (c) oxygenated blood and (d) deoxygenated blood.